CONF-900917--27

WSRC-RP--89-1422

DE91 004273

A1-U FUEL FOAMING/RECRITICALITY CONSIDERATIONS FOR PRODUCTION REACTOR CORE-MELT ACCIDENTS (U)

by

A. W. Cronenberg
Engineering Sciences and Analysis
8100 Mountain Road, NE
Albuquerque, NM 87110

M. L. Hyder, and P. G. Ellison
Westinghouse Savannah River Company
Savannah River Site
Aiken, South Carolina 29808

A paper for presentation at

The ANS International Topical of Safety of
Non-Commercial Reactors Conference
Boise, Idaho
Sept. 30-Oct.4, 1990

and publication in the Conference Proceedings

Signature 5/29/90
Date

Al-U FUEL FOAMING/RECRITICALITY CONSIDERATIONS FOR PRODUCTION REACTOR CORE-MELT ACCIDENTS

A. W. Cronenberg
Engineering Science and Analysis
8100 Mountain Road, NE
Albuquerque, NM 87110

M. L. Hyder, and P. G. Ellison
Westinghouse Savannah River Company
Savannah River Site
Aiken, SC 29808
803-725-4188

ABSTRACT

Severe accident studies for the Savannah River production reactors indicate that if coherent fuel melting and relocation occur in the absence of target melting, in-vessel recriticality may be achieved. In this paper, fuel-melt/target interaction potential is assessed, where fission gas-induced fuel foaming and melt attack on target material are evaluated and compared with available data. Models are developed to characterize foams for irradiated Al-based fuel. Predictions indicate transient foaming (the extent of which is governed by fission gas inventory), heating transient, and bubble coalescence behavior. The model also indicates that metallic foams are basically unstable and will collapse, which largely depends on film tenacity and melt viscosity. For high-burnup fuel, foams lasting tens of seconds are predicted, allowing molten fuel to contact and cause melt ablation of concentric targets. For low-burnup fuel, contact can not be assured, thus recriticality may be of concern at reactor startup.

INTRODUCTION

The primary purpose of the Savannah River Site (SRS) reactors is the production of tritium for national defense. For over 30 years this mission has been conducted without serious threat to the public; nevertheless, post-Chernobyl concerns regarding the safety of Department of Energy (DOE) reactors has heightened issues with regards to severe accident consequences. To provide continued assurance that the SRS reactors can be operated without undue risk, DOE has initiated a program to upgrade present and future production reactors to the highest safety standards. A central part of this program involves the understanding of governing phenomena and ability to quantify the consequences of low-probability/high-consequence accidents involving core meltdown.

For severe accidents the issue of recriticality is of concern, where core-melt relocation in the presence of a water moderator may, under certain conditions, lead to recriticality. Such recriticality is possible for coherent fuel melting and relocation in the absence of target melting. Mixing of target and fuel melt, however, will assure a non-critical configuration. It is of interest therefore to assess fuel/target interaction potential, where the influence of fission-gas-induced fuel swelling/foaming behavior are primary mechanisms for fuel-melt attack of targets. In this paper, models are developed for the prediction of irradiated fuel foaming and foam stability characteristics. Calculation results are applied to SRS Mark-22 concentric fuel/target geometry and illustrated in Figure 1. Predicted trends are compared with experimental observations on irradiated fuel foam characteristics and conclusions given with respect to recriticality concerns.

M9005018

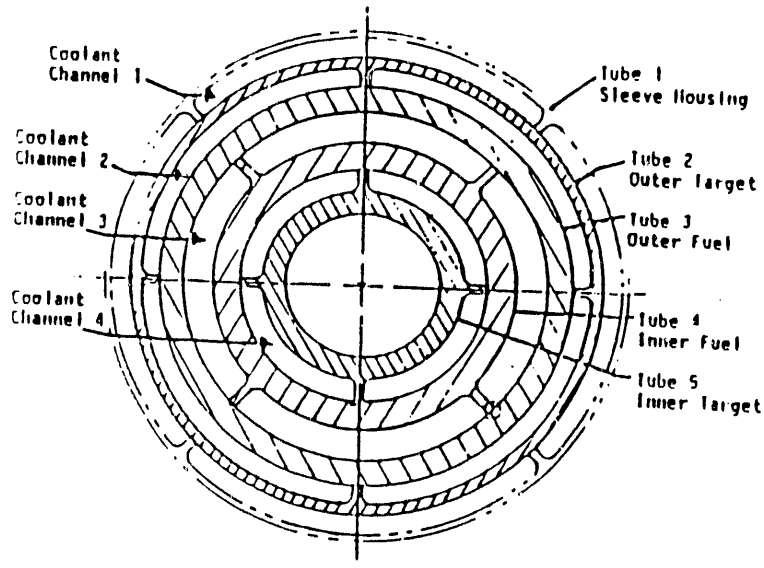

Figure 1. Illustration of Mark-22 Fuel/Target Assembly

FOAM CHARACTERIZATION

Simply stated, a foam is an agglomeration of gas bubbles separated from each other by a network of thin liquid films. Bubble morphology characteristics largely govern the extent of foaming, while the tenacity of the film network controls foam stability. For irradiated fuel, the foaming potential largely depends on changes in the morphology of entrapped fission gas bubbles as the fuel melts, while foam stability is governed by the persistence of the liquid films separating the gas phase from the melt.

Figure 2 illustrates the sequence of events involved in spontaneously induced foaming for irradiated nuclear fuel[1]. Initially, fission gas is imbedded in the fuel matrix as individual atoms, followed by nucleation of micro-bubbles within the fuel matrix. Upon fuel melting, enhanced bubble coalescence, expansion, and attendant fuel swelling occur. If coalescence is rapid, the foamed state can be reached. If bubble coalescence is slow, bubble escape at the free surface may prevent the highly voided condition necessary for true foaming. Thus, foaming is largely a race between bubble nucleation, growth, and coalescence versus gas escape from the melt.

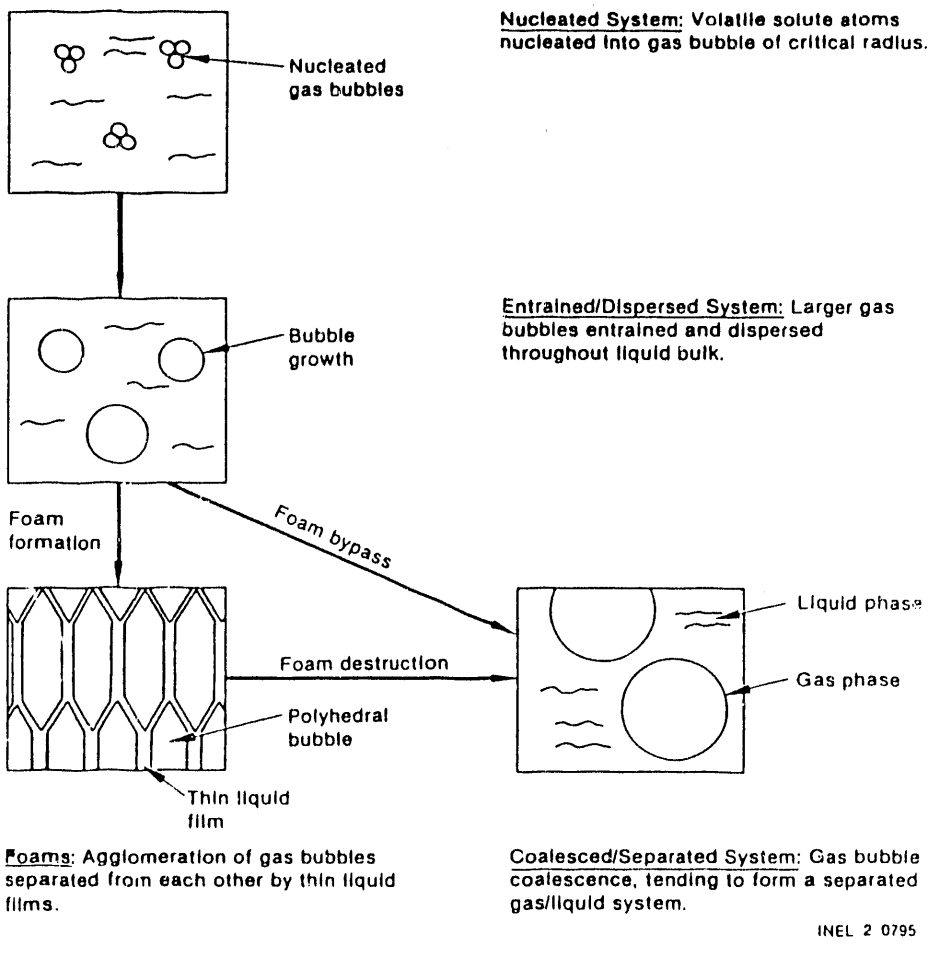

Figure 2. Illustration of Sequence of Events Associated With Irradiated Fuel Foam Formation and Destruction

Once formed, foams will tend to collapse due to film destruction. Drainage of the intervening film between two adjacent bubbles will lead to foam collapse. Quantitative models for the assessment of foam formation and stability characteristics are presented in this paper and applied to SRS conditions.

Foam Inducement

The extent of foaming for irradiated fuel upon melting can be calculated as the sum of several contributions associated with the expansion of the fuel upon melting and changes in bubble morphology within the melt; i.e.:

$$F_{total} = F_{matrix} + F_{st} + F_{bc} + F_{th} \quad (1)$$

where F_{matrix} is the expansion of the fuel cell upon melting, F_{st} is the change in bubble volume resulting from the lowered surface tension upon solid-to-liquid phase transformation, F_{bc} is the volumetric expansion resulting from bubble coalescence, F_{th} is thermally induced bubble growth, and the fractional extent of volumetric swelling (F) for an individual mechanism can be expressed as:

$$F = (V_{final} - V_{initial})/V_{initial} \quad (2)$$

where V is the volume of a unit fuel cell (i.e., 1 cm^3).

Fuel matrix expansion upon melting can be estimated as:

$$F_{matrix} = (\rho_s/\rho_m) - 1 \quad (3)$$

where ρ_s and ρ_m are the densities of the solid and melt respectively.

Noting that the aluminum density at room temperature is about 2.7 g/cm^3 versus 2.38 g/cm^3 at melting, the volumetric swelling resulting from density changes is about 13 percent.[a]

The influence of a reduction in surface tension (σ) on the volume occupied by fission gas bubbles in the melt versus solid can be assessed from the the following equilibrium force balance:

$$(2\sigma_s + PR_s)R_s^2 = (2\sigma_m + PR_m)R_m^2 \quad (4)$$

where P is ambient pressure, and σ_s and σ_m are, respectively, the solid and melt surface tension.

---

a. F_{matrix} is dependent on UAl_x alloying composition, where little expansion is expected upon melting for high U content resulting from reduced ρ_s with increased U.

Solving equation (4) for R_m, the fractional swelling caused by changes in surface tension is:

$$F_{st} = \frac{N(4\pi/3)[R_m^3 - R_s^3]}{1 + N(4\pi/3)R_s^3} \quad . \tag{5}$$

The bubble concentration (N, bubbles/cc-fuel) can be estimated as:

$$N = N_g/N_{gb} \tag{6}$$

where N_g is the number of gas atoms per unit volume, N_{gb} is the number of gas atoms per bubble (R) and R is estimated from the equation of state for microbubbles [2], which is:

$$N_{gb} = \frac{V_b}{[A = BR]} \tag{7}$$

where V_b equals bubble volume, A equals 85 E-24 cm^3, B equals $kT/2\sigma$, k equals Boltzmann's constant, and T equals temperature.

As shown in Table 1, surface tension effects on swelling are quite limited and estimated to contribute a maximum volumetric swelling of about ten percent for large bubbles (20,000 A°) associated with high-burnup conditions (50 atom-percent). At lower burnups and smaller bubble radii, the effect is much lower. Because a three-fold volumetric swelling is required to ensure good fuel/target contact for Savannah River Mark-22 assemblies, changes in fuel density and surface tension upon melting are not sufficient to account for fuel/target contact. The primary mechanisms for foam inducement, therefore, relate to changes in bubble morphology caused by enhanced bubble coalescence in the melt and thermally induced bubble expansion.

Upon fuel melting, an increase in bubble mobility occurs, inducing coalescence of numerous microbubbles into fewer but larger bubbles with attendant fuel swelling. Coalescence will result in continued bubble growth and fuel swelling until large bubbles try to escape from the melt by bouyancy-driven forces or other bubble escape mechanisms. Thus, the extent of foaming can be viewed as largely a race between bubble coalescence versus escape, which can be assessed by determination of the critical bubble radius (R_c) at which bouyancy-induced bubble escape just matches that of bubble migration/coalescence by volume diffusion, i.e.:

$$R_c = [(9/8\pi)(1/\rho g)(Q/r_a)(\Delta T/T)]^{0.5} \tag{8}$$

where ΔT equals temperature gradient, T equals temperature, Q equals activation energy for volume diffusion, r_a equals atomic radius, ρ equals melt density, and g equals gravitation constant.

TABLE 1. Swelling Caused by Surface Tension Effects

Parameter Values

σ_s = 1000 dy/cm
σ_m = 914 dy/cm
P = 1 atm (1.0E+6 dy/cm^2)
N_g = 2.0 E+20 gas-atoms/cc-fuel (at 50-percent atom burnup)

Calculation

$R_{b,s}$, A° (cm)	$R_{b,m}$, A°	N, bubbles/cc	F_{st}, percent
10 (1.0E-7)	10.46	4.44 E+18	0.26
200 (2.0E-6)	209	1.41 E+15	0.64
1000 (1.0E-5)	1045	4.01 E+13	2.03
10,000 (1.0E-4)	10,440	3.64 E+11	8.10
20,000 (2.0E-4)	20,830	9.07 E+10	9.75

For SRP core-meltdown conditions, R_c is estimated to be in the range of 20,000 A°. Coalescence to a limit of 20,000 A° is based on equilibrium betgween escape and coalescence; while, at transient heating conditions, a non-equilibrium condition exists so that larger bubble radii can be expected, thus, equation (8) yields a lower limit of coalescence.

The fractional swelling per unit fuel volume caused by a change in bubble morphology by coalescence can be expressed as:

$$F_{bc} = \frac{(4\pi/3)[N_2R_2^3 - N1R_1^3]}{1 + N_1(4\pi R_1^3/3)} \quad \text{and} \quad R_2 = R_c \qquad (9)$$

where the subscripts 1 and 2 refer to the initial (uncoalesced) and final (coalesced) states respectively.

A similar expression for fractional swelling (F_{th}) resulting from an increase in fuel temperature can be defined, where, in this case, the bubble density (N) remains constant and ideal gas behavior is assumed, i.e.:

$$F_{th} = \frac{N(4\pi/3)(R_2^3 - R_c^3)}{1 + N(4\pi R_c^3/3)} \quad \text{and} \quad R2 = [(T_2T_1)R_C^2]^{0.5} \tag{10}$$

where R_c is the critical bubble radius for coalescence in the melt before thermally induced bubble expansion.

Calculation results [as a function of fuel temperature (1,000 and 1,500 K), burnup (50, 5, and 1 atom-percent), and extent of bubble coalescence (R_c = 20,000 - 30,000 A°)] are summarized in Table 2, where R_1 equals 10 A° and T_1 equals 500 K, which is characteristic of normal SRP operational conditions. Results indicate that at elevated burnup (50 atom-percent) and temperature (1000 - 1500 K), a five-to-eight-fold increase in volumetric swelling can be expected so that Mark-22 fuel/target contact is assured (i.e., a three-fold increase in fuel melt volume is required for fuel/target contact. However, at reduced burnups and associated limited gas inventory conditions, the predicted extent of fuel swelling/foaming is insufficient to cause fuel/target contact. It is also interesting that temperature gradient effects are of importance, where enhanced bubble mobility/coalescence is predicted at increased gradients as demonstrated in Equation (8) where increased ΔT yields larger R_c. The foaming potential would thus be enhanced for increased transient heating conditions.

Foam Stability

Although large-scale foaming is predicted for high burnup, the question arises as to the stability characteristics of such metallic foams and whether sufficient time exists for target melting. The characteristic time for target melting can be approximated from the following equation for the thermal relaxation period:

$$t_{t,m} \simeq X^2/(\alpha a^2) \tag{11}$$

where α equals thermal diffusivity, X equals target thickness, and a equals solidification constant assessed from equation (12).

$$C_p(T_{mp} - T)/L \simeq a \exp(a^2) \tag{12}$$

where C_p equals specific heat, T_{mp} equals melting point, T equals initial target temperature, and L equals the latent heat of fusion.

Table 3 indicates that for Al-based targets and Mark-22 geometry, a thermal relaxation time of 1.3 seconds (s) is estimated. Thus, fuel foam must be stable for several seconds in order to initiate target melting.

TABLE 2. Summary of Predicted Foaming Behavior of Irradiated U-Al Fuel

Initial Conditions: $R_1 = 10$ A° $T_1 = 500$ K

Burnup (percent)	Temperature T_2 (K)	Fractional Bubble Coalescence (F_{bc} at Rc)	Fractional Bubble Thermal Expansion (F_{th})	Total Volumetric Swelling (F_t)
50	1000	2.97 (20,000 A°)	2.79	5.76
	1500	2.97 (20,000 A°)	5.64	8.61
	1000	4.45(30,000 A°)	1.50	5.97
	1500	4.45 (30,000 A°)	3.44	7.89
5	1000	0.30 (20,000 A°)	0.43	0.73
	1500	0.30 (20,000 A°)	0.98	1.28
	1000	0.45 (30,000 A°)	0.57	1.02
	1500	0.45 (30,000 A°)	1.31	1.76
1	1000	0.06 (20,000 A°)	0.10	0.16
	1500	0.06 (20,000 A°)	0.24	0.30
	1000	0.09 (30,000 A°)	0.15	0.24
	1500	0.09 (30,000 A°)	0.35	0.44

$\overline{F_t \simeq F_{bc} + F_{th}}$

Table 3. Estimated Target Thermal Relation Time

Parameter Values (Al-melt)

C_p	= 0.26 cal/g-K	k	= 0.25 cal/s-cm-K
T_{mp}	= 933 K	ρ	= 2.38 g/cm^3
T	= 600 K	α	= $k/\rho C_p$ = 0.4 cm^2/s
L	= 95 cal/g	a	= 0.62

Calculation

$C_p(T_{mp} - T)/L = 0.91$

X(Mark-22 inner target) = 2.019 cm - 1.57 cm = 0.449 cm

$t_{t,m} \simeq X^2/(\alpha a^2) \simeq 1.3s$

To evaluate foam stability characteristics, the time scale for thinning/destruction of the film lamellae between two large coalesced bubbles is assessed for the geometry illustrated in Figure 3, where the velocity profile is based on the solution of the Navier-Stokes equation for film flow as developed by Lee and Hodgson[3].

$$V(r,z) = \frac{\Delta P}{\mu}\left[\left(\frac{h}{2}\right)^2 - z^2\right](r/R_f^2) \qquad (13)$$

where h equals film thickness, ΔP equals pressure differential, and R_f equals radius of film disk. Application of mass continuity for the rate of film thinning in the Z and r directions yields the following relationship[4].

$$-\frac{dh}{dt} = \frac{h^3 \Delta P}{3\mu R_f^2} \qquad (14)$$

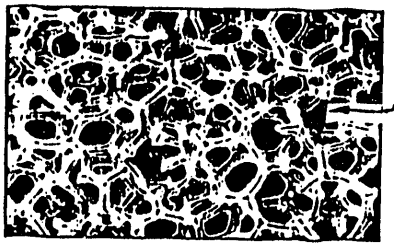

Destruction of Film Network Induces Foam Collapse

Foam Morphology With Characteristic Thin Film Lamellae

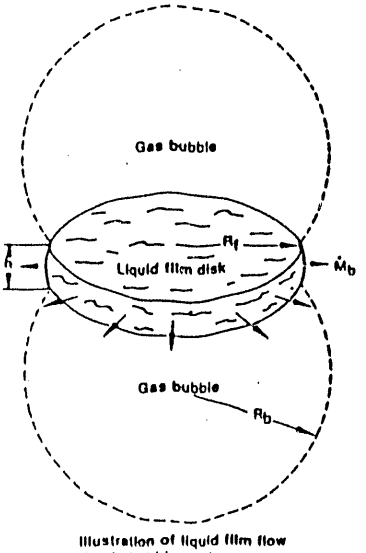

Illustration of liquid film flow due to bubble coalescence

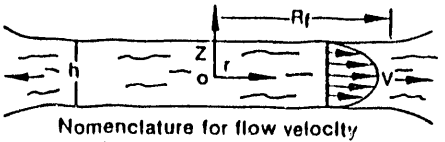

Nomenclature for flow velocity profile in liquid film disk using a rigid-wall, parallel-plate model

INEL 2 0794

Figure 3. Film Thinning Model Between Two Large Coalesced Bubbles at Onset of Foam Destruction.

This relationship, upon integration from the original film thickness (h_o) to the critical thickness (h_c) at which film destruction occurs, yields the time for film destruction by thinning[4].

$$\int_{h_o}^{h_c} -h^{-3}\, dh = \frac{\Delta P}{3\,\mu\, R_f^2} \int_{o}^{t_t} dt \quad \text{and} \tag{15}$$

$$t_t = \frac{3\,\mu\, R_f^2}{2\,\Delta P} \left(\frac{1}{h_c^2} - \frac{1}{h_o^2}\right) \tag{16}$$

Because $h_o >> h_c$, the film destruction time can be approximated as:

$$t_t \simeq \frac{3\,\mu\, R_f^2}{2\,\Delta P\, h_c^2} \tag{17}$$

It is interesting that the film thinning time is essentially independent of the original film thickness, but rather depends on the length of the film ligament (R_f) and the critical film thickness (h_c) at which rupture occurs. For practical purposes $R_f \simeq R$ (bubble radius), while the pressure differential on vertical film lamellae can be approximated as $\Delta P \simeq 2R\rho g$, thus:

$$t_t \simeq \frac{3\,\mu\, R}{4\rho g h_c^2} \tag{18}$$

where ρ is the melt density and g is the gravitation constant (980 cm/s^2).

Several criteria have been suggested for estimation of h_c [5]. DeVries [6] proposed that rupture of film lamellae occur by wave instabilities at thickness of about 100 A°. In a nuclear radiation environment, puncturing of films by fission-fragment ionization (stopping length of 1000 A°)[7] may be a more appropriate criteria for h_c.

Table 4 presents predicted film thinning times at various h_c and final coalesced bubble radii. As indicated, the film drainage time (and thus foam stability) is largely controlled by the critical thickness (h_c) at which film rupture occurs. If film thinning down to 100 A° occurs, then drainage times on the order of 20 minutes are estimated. In a radiation field (h_c = 1000 A°), a much shorter time is estimated (i.e., $t_t \simeq$ 10s).

Table 4. Estimated Film Destruction Times

Parameter Values, Al-melt

$\mu = 0.015$ g/s-cm $\quad \rho = 2.38$ g/cm^3

$g = 980$ cm/s^2 $\quad 3\mu/4\rho g = 4.823$ E-6 cm-s

Bubble Radius, R (A°)	Critical Film Thickness, h_c (A°)	Film Thinning Time, t_t (s)
20,000	100	964 (≃ 16 min)
	1000	9.64
30,000	100	1447 (≃ 24 min)
	1000	14.47

DISCUSSION AND COMPARISON WITH EXPERIMENTAL OBSERVATIONS

The results of the foregoing analysis indicate some of the essential features of foam formation and stability for irradiated nuclear fuel. Of particular note is the overriding dependance of the foaming potential on fission gas inventory and the extent of bubble coalescence as revealed by equations (9) and (10). Fuel at low fission gas inventory and corresponding low bubble concentrations (N) exhibit limited foaming potential. The extent of volumetric foaming is also largely determined by bubble morphology conditions: that is, the amount of bubble coalescence (R_c) and thermally induced bubble expansion. The more pronounced the extent of bubble coalescence, the greater the volumetric swelling; thus, at a particular burnup condition, larger but fewer bubbles will lead to greater foaming than numerous but smaller bubbles. It is from this perspective that foaming can be viewed largely as a race between coalescence and fission gas bubble escape from the melt.

In the analysis presented, the limit of bubble coalescence (i.e., critical bubble radius, R_c) was defined using two criteria. The first is based on the condition of equilibrium between bouyancy-induced bubble escape from the melt versus coalescence by a volume diffusion mechanism. Such a coalescence limit does not account for other contributions to bubble mobility (e.g., evaporation/condensation, stress-induced bubble mobility, sweeping of gas atoms by bubbles) or the various factors that contribute to gas escape from the melt (e.g., interlinking of bubbles, melt breakup). Thus, predicted values of the coalescence limit (R_c) are approximate and represent a lower limit of coalescence. Nevertheless, a five-to-eight-fold increase in volumetric foaming is predicted for SRS fuel at 50 atom-percent burnup and coalescence to bubble radii of 20,000 to 30,000 A°. A decrease in fission gas inventory by a factor of ten (burnup equals 5 atom-percent) results in less than a two-fold increase in swelling at similar bubble radii. Thus, fission gas inventory (burnup) conditions are the single most important factor governing fuel foaming potential.

Although extensive foaming is predicted for high-burnup aluminum-based fuel, such metallic foams are unstable and collapse as a result of destruction of the thin film lamellae that constitute the

film network characteristic of the foamed condition (Figures 2 and 3). The time scale for film destruction was characterized from consideration of gravity-induced film drainage, where thinning to a critical film thickness (h_c) results in film destruction and onset of foam collapse. Predicted film thinning times exhibit a 2ed power dependence on h_c; thus, foam stability is considered largely dependent on the film thickness (h_c) as film rupture occurs. For a radiation environment, film puncturing by ionization at $h_c \simeq 1000$ A° yields an onset time of foam collapse of tens of seconds. In a non-radiation environment, films are considered stable to 100 A° with corresponding film thinning times on the order of tens of minutes.

Although the modeling approach outlined is approximate and considers only first order effects; nevertheless, it serves as a basis for prediction of overall trends. These trends are compared here with experimental observations. Revealing experiments are those conducted in the early 60's by Buddery and Scott [8], where fission gas release and swelling of molten U-metal was examined. Natural uranium samples were heated out-of-pile to uranium-melting temperatures (T_{mp} = 1405 K) at fission gas densities of about 2.0 E+19 gas-atoms per cc-fuel (corresponds to about five-percent burnup for SRS fuel). Transient swelling and collapse behavior was characterized from fuel volume and density estimates, which are plotted in Figure 4 in terms of fuel-specific volume. Initial swelling is evident with subsequent collapse upon fission gas release from the melt. More than 99 percent of the Kr^{85} (measured during testing) was lost on melting. Rapid gas release began about 10^0C below the melting point and increased once melting occurred. The final configuration was a once-molten pool of almost full-density uranium covered by a low-density froth.

Based on such observation Buddery and Scott [8] concluded that, for irradiated metallic fuel, initial foaming behavior can be expected, followed by rapid froth collapse upon release of previously entrapped fission gas. The final density of the fuel can be expected to be close to that of the initial density prior to heating. They also concluded that although burnup and melt temperature had a large impact on the extent of foaming, these parameters had little effect on the rate of gas release and foam collapse. Such experimental observations are in general agreement with predicted modeling trends (i.e., initial foaming at fuel melting with subsequent foam collapse upon release of entrapped fission gases). It is interesting that the half width of the swelling/collapse peak shown in Figure 4 is on the order of 15 seconds. This experimental value compares favorably with the film destruction times (foam collapse) estimated in Table 4.

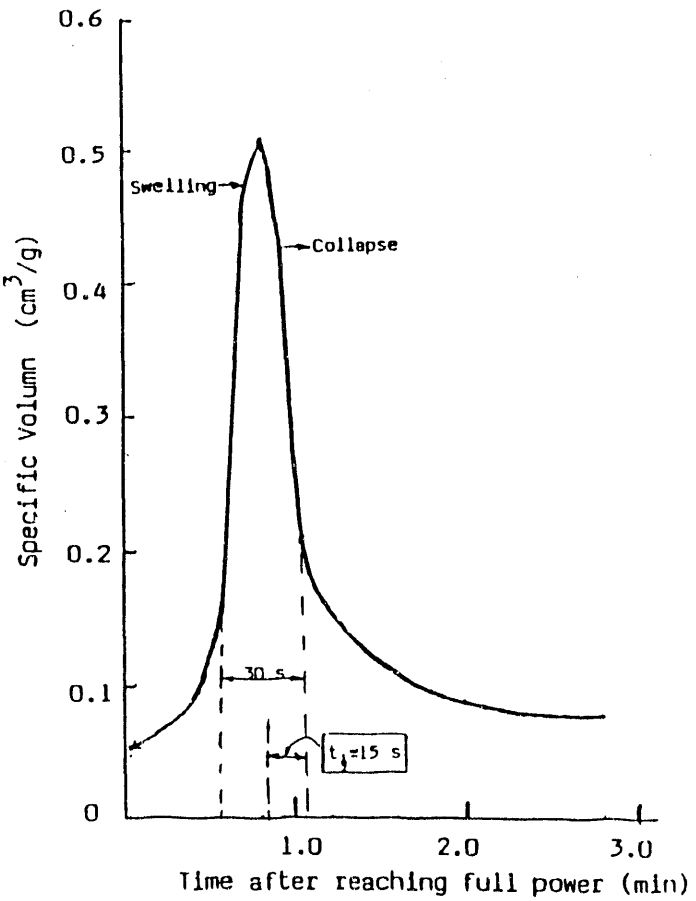

Figure 4. Experimental Swelling/Foaming Behavior Noted for Previously-Irradiated U-metal Fuel Brought to Melt Temperatures.

CONCLUSIONS

Models of transient foaming and collapse behavior for irradiated metallic fuel heated to melt temperatures indicate that the foaming potential is governed by fission gas inventory conditions. Fuel at low fission gas inventory and corresponding low bubble concentrations exhibit limited foaming potential; whereas high-burnup fuel exhibits a high potential to foam. The actual extent of volumetric

CONCLUSIONS

foaming, however, is largely determined by bubble morphology conditions, (i.e., the amount of bubble coalescence and thermally induced bubble expansion). The more pronounced the extent of bubble coalescence, the greater the volumetric swelling; thus, at a particular burnup condition, larger but fewer bubbles will lead to greater foaming then numerous but smaller bubbles. Fuel foaming can therefore be viewed largely as a race between coalescence and fission gas escape from the melt.

Although extensive foaming is predicted for high-burnup, aluminum-based fuel, such metallic foams are predicted to be unstable and collapse because of destruction of the thin film lamellae that constitute the film network characteristic of the foamed state. The timing of collapse will depend on several factors, including the film thickness at which rupture occurs, melt geometry, and viscosity. U-Al foams lasting tens of seconds are predicted for radiation environments resulting from film ionization at a thickness of 1000 A°, while longer foam lifetimes are predicted for non-radiation environments (tens of minutes) where films are considered stable to 100 A°.

For SRS Mark-22 geometry, fuel foaming at high-burnup conditions is sufficient to induce fuel melt contact with target material and remain stable for tens of seconds, which would allow for onset of target melting. For low-burnup SRS fuel, fuel/target contact can not be assured, so recriticality may be of concern at reactor startup conditions.

REFERENCES

1. A. W. CRONENBERG, D. W. CROUCHER, AND P. E. MACDONALD, "Fuel Foaming and Collapse During LWR Core Meltdown Accidents", J. Nucl. Tech., 312-325 (1984).

2. D. OLANDER, *Fundamental Aspects of Nuclear Reactor Fuel Elements,* Publication, 204 (1976).

3. J. C. LEE AND T. D. HODGSON, "Film Flow and Coalescence: Basic Relations, Film Shape, and Criteria for Interface Mobility," *Chemical Enginering Science,* 23 1375-1397 (1968).

4. A. W. CRONENBERG, D. W. CROUCHER, AND P.E. MACDONALD, "An Assessment of Fuel Foaming Potential During Core Meltdown Accidents," NUREG/CR-2701, EGG-2191, (Oct. 1982).

5. I. L. JASHNANI AND R. LEMLICH, "Foam Drainage, Surface Viscosity, and Bubble Size Bias", Colloidal and Interfacial Science (46), 13-16, (1974).

6. A. J. DEVRIES, Foam Stability, Delft, The Netherlands, Rubber-Stichting Publishing Company (1957).

7. J. H. CHUTE, "Direct Observations of Fission Fragment Damage in Ceramic Oxides," *Journal of Nuclear Material*, 21, 77-87 (1967).

8. H. BUDDERY AND K. T. SCOTT, "A Study of The Melting of Irradiated Uranium", *Journal of Nuclear Material*, 5, 81-93 (1962).

DISCLAIMER

END

DATE FILMED

12/12/90